Journal of Statistical Physics, Vol. 67, Nos. 5/6, 1992

Chaotic and Self-Organized Critical Behavior of a Generalized Slider-Block Model

Galina Narkounskaia,[1] Jie Huang,[1] and Donald L. Turcotte[1]

Received August 19, 1991; final January 3, 1992

The dynamical behavior of two-dimensional arrays of slider blocks is considered. The blocks are pulled across a frictional surface by a constant-velocity driver; the blocks are connected to the driver and to each other by springs. Only one block is allowed to slip at a time and its displacement can be obtained analytically; the system is deterministic with no stochastic inputs. Studies of a pair of slider blocks show that they exibit periodic, limit-cycle, or choatic behavior depending upon parameter values and initial conditions. Studies of large, two-dimensional arrays of blocks show self-organized criticality. Positive Lyapunov exponents are found that depend upon the stiffness and size of the array.

KEY WORDS: Chaos; self-organized criticality.

1. INTRODUCTION

Since chaotic behavior of deterministic systems was first discovered by Lorentz[1] a large number of problems have been shown to exhibit deterministic choas. Chaotic behavior has been found for both iterative maps and sets of differential equations. However, studies of chaotic behavior have generally been restricted to low-order systems. For this reason the number of applications in continuum mechanics has been quite limited.

As an approach to large interative systems, Bak *et al.*[2] proposed a simple cellular-automata model for self-organized criticality. Particles were randomly added to a square grid of boxes, and when a box had four particles, they were redistributed to the four adjacent boxes. If after a redistribution from a box any of the adjacent boxes had four or more particles, further redistributions were required. On average, all particles

[1] Department of Geological Sciences, Cornell University, Ithaca, New York 14853.

0022-4715/92/0600-1151$06.50/0

added were lost from the boundaries of the grid. The behavior of the system was characterized by the statistical frequency–size distribution of events, which was found to be a power-law (fractal) relation.

In this paper we will consider a slider-block model that exhibits chaotic behavior at low order and self-organized criticality at high order. A multiple slider-block model was introduced by Burridge and Knopoff[3] as an analog for earthquakes. A constant-velocity driver was attached to one or more blocks by springs. The blocks interact with a surface resulting in a frictional resistance; if the dynamic friction is less than the static friction or if a velocity-weakening friction law is used, stick-slip behavior is observed. Huang and Turcotte[4] showed that a pair of slider blocks often behaved in a chaotic manner as long as the system was asymmetric, i.e., the blocks had different masses. The period-doubling route to chaos was observed and it satisfied the Feigenbaum relation.

Carlson and Langer[5] considered a linear array of slider blocks; each block was attached by springs to a constant-velocity driver and to its nearest neighbors. They found that the statistical frequency–size distribution of small events was a power law (fractal), but an anomalously large number of events occurred that included all blocks. They suggested that their system behaved chaotically and exhibited self-organized criticality. Ito and Matsuzaki[6] discussed the strong similarities between cellular-automata and slider-block models. Nakanishi[7] modified the multiple-slider-block model so that only the block or blocks that are initially unstable are allowed to slide. The transfer of stress may destabilize adjacent blocks and these are allowed to slide subsequently. A modification of this model was applied to a two-dimensional array of blocks by Brown *et al.*[8]

In this paper we will consider a generalized slider-block model which combines various aspects of previous models. We will study both low-order and high-order systems and will determine whether the behavior is chaotic.

2. GENERAL MODEL

Our generalized dynamical system consists of N blocks that are pulled across a frictional surface by a driver moving at a constant velocity v. The blocks are loaded in the x direction and there are no displacements in the y direction. Block i with mass m_i is connected to the driver by a spring; the spring constant is k_{ii} and its extension is x_i. Each pair of blocks is connected to each other with a spring; the spring constant is k_{ij} and its extension is $x_j - x_i$. The motion of block i is reatarded by the frictional force F_i. A simplified version consisting of four blocks is illustrated in Fig. 1. We will assume that the velocity of the driver is small, so we can neglect the displacement of the driver relative to the surface during a slip

event. We also assume a static–dynamic friction law. Each block sticks until the elastic force applied to it is $\geqslant$ the static friction F_{si}. It then slips until its velocity relative to the surface is equal to 0. The dynamic friction during the slip is $F_{di} = \xi F_{si}$, where the parameter ξ is the ratio of dynamic to static friction; stick-slip behavior requires that $\xi < 1$.

The failure condition for block i is

$$k_{ii} x_i - \sum_{j \neq i} k_{ij}(x_j - x_i) \geqslant F_{si} \tag{2.1}$$

where the left-hand side is the sum of the forces transmitted to the block by the driving and connecting springs. Slip commences when condition (2.1) is violated. The equation of the motion of block i during slip is

$$m_i \ddot{x}_i = -k_{ii} x_i + \sum_{j \neq i} k_{ij}(x_j - x_i) + F_{di} \tag{2.2}$$

Let $m_i = \gamma_i m$; $k_{ij} = \alpha_{ij} k$ and $F_{si} = \beta_i F$, where α_{ij} is a stiffness parameter and represents the relative strength of the coupling and driver springs. We introduce dimensionless variables $X_i = x_i k/F$, $\tau = t(k/m)^{1/2}$, and denote $\theta_i = \sum_{j=1}^{N} \alpha_{ij}$. The dimensionless failure condition for block i is

$$X_i \theta_i - \sum_{j \neq i} \alpha_{ij} X_j \geqslant \beta_i \tag{2.3}$$

The dimensionless equation of motion for block i is

$$\gamma_i \ddot{X}_i + X_i \theta_i - \sum_{j \neq i} \alpha_{ij} X_j = \xi \beta_i \tag{2.4}$$

Let $(a_1, a_2, \ldots, a_N)$ be a solution of the system of N linear equations

$$a_i \theta_i - \sum_{j \neq i} \alpha_{ij} \alpha_j = \beta_i, \qquad \text{for} \quad i = 1, \ldots, N \tag{2.5}$$

Let $C = (c_{ij})$ be the matrix of the coefficients of the system (2.5), where $c_{ij} = -\alpha_{ij}$ for $i \neq j$ and $c_{ii} = \theta_i$. We will prove that $\det(C) \neq 0$ if we have nonzero loading spring coefficients α_{ii}. It follows from this statement that the linear system (2.5) always has a unique solution. Assume that $\det(C) = 0$. We consider rows of C as vectors $\mathbf{v}_i = (c_1, c_{i2}, \ldots, c_{iN})$. The statement that C is degenerate is equivalent to the statement that there is a nonzero linear combination of $\mathbf{v}_i$ equal to 0, i.e., there are N real numbers d_i, not all equal to 0, such that $\sum_{i=1}^{N} d_i \mathbf{v}_i = 0$. Thus, for the matrix coefficients of C we have

$$\sum_{i=1}^{N} d_i c_{ij} = 0 \qquad \text{for} \quad j = 1, \ldots, N \tag{2.6}$$

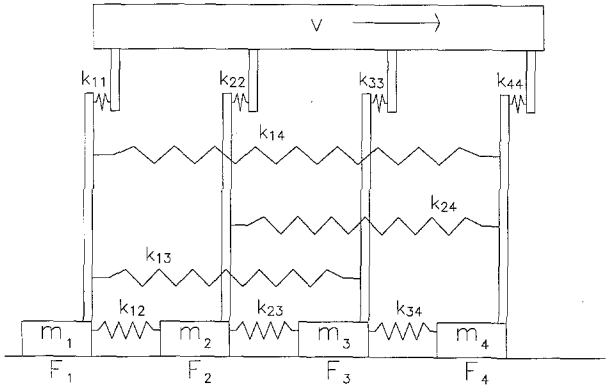

Fig. 1. Illustration of our generalized slider-block model. A constant-velocity (v) driver pulls blocks of mass m_i across a surface. The masses are attached to the driver by springs with spring constants k_{ii} and to each other by springs with spring constants k_{ij}. The motion is retarded by the frictional forces F_i.

Let i_1 be such a number that $|d_{i_1}| = \max_{i=1,\ldots,N} |d_i|$. We can assume that $d_{i_1} > 0$, otherwise we can change the sign of all d_i. We take $j = i_1$ in (2.6), put the term in the sum with $i = i_1$ separately, and use the condition that $\alpha_{ij} = \alpha_{ji}$ and the definition of c_{ij},

$$d_{i_1}\alpha_{i_1 i_1} + d_{i_1}\sum_{i\neq i_1}\alpha_{i_1 i} - \sum_{i\neq i_1} d_i\alpha_{ii_1} = d_{i_1}\alpha_{i_1 i_1} + \sum_{i\neq i_1}(d_{i_1} - d_i)\alpha_{ii_1} \tag{2.7}$$

In (2.7) the first term on the right side is positive and the sum is non-negative, so that (2.7) is positive, but it must be equal to 0, so we have a contradiction and our assumption is wrong and we always have a unique solution.

Now we will prove that the evolution of our system does not depend on the dynamic friction. Taking $\xi = 0$, we can write (2.4) as

$$\gamma_i \dot{X}_{i0} + X_{i0}\theta_i - \sum_{j\neq i}\alpha_{ij}X_{j0} = 0 \tag{2.8}$$

The failure conditions are still (2.3). We introduce a linear change of variables

$$X_i = a_i + (1-\xi)(X_{i0} - a_i) \tag{2.9}$$

From (2.8) and (2.9) it follows that

$$X_{i0} = a_i + \frac{X_i - a_i}{1-\xi} \tag{2.10}$$

and

$$\gamma_i \ddot{X}_i/(1-\xi) + X_i\theta_i/(1-\xi) - \left(\sum_{j\neq i} \alpha_{ij} X_j\right)\Big/(1-\xi)$$
$$+ a_i\theta_i[1-1/(1-\xi)] - \left(\sum_{j\neq i} \alpha_{ij} a_j\right)[1-1/(1-\xi)] = 0 \quad (2.11)$$

Since $a_i\theta_i - \sum_{j\neq i} \alpha_{ij} a_j = \beta_i$, we multiply (2.11) by $(1-\xi)$ and have the following equations for X_i {we use that $[1-1/(1-\xi)](1-\xi) = -\xi$}:

$$\gamma_i \ddot{X}_i + X_i\theta_i - \left(\sum_{j\neq i} \alpha_{ij} X_j\right) - \xi\beta_i = 0 \quad (2.12)$$

which is equivalent to (2.4). Substitution of (2.10) into (2.3) gives the same failure criteria for X_i as for X_{i0}. So the linear change of variables transfers the system with zero dynamic friction into the system with any other ratio of dynamic to static friction; therefore we will take $\xi = 0$ in the results presented below. It is interesting to note that when $\xi = 0$ no energy is lost through frictional dissipation and the average force exerted on the constant-velocity driver is zero. At some times it is necessary to pull the driver and store energy in the springs, at other times the springs push the driver and the stored energy decreases.

We will further require that only one block can move at a time. All others stick until the first one stops. Then a second block will be allowed to move if its failure criterion is violated and so on until the failure criterion is satisfied by all blocks. Then we will have a period of strain accumulation until the next event begins. Each event consists of several consecutive slips of different blocks. Let $d_i^{k,0}$ be the displacement of block i before event k and $d_i^{k,j}$ be the displacement of block i after the slip j in event k. The vector $\mathbf{d}^{k,j} = (d_1^{k,j}, d_2^{k,j}, \ldots, d_N^{k,j})$ gives us the state of the system after slip j in event k, and a trajectory in the displacement phase space is a piecewise linear curve with vertices $\mathbf{d}^{k,j}$.

We next find the dependence of $\mathbf{d}^{k,j+1}$ on $\mathbf{d}^{k,j}$. Let block m move in slip $(j+1)$ of event k. Then $d_i^{k,j+1} = d_i^{k,j}$ for $i \neq m$. Denote $\eta_m = \sum_{i\neq m} \alpha_{mi} d_i^{k,j}$ and $\lambda = (\theta_m/\gamma_m)^{1/2}$. The displacement of block m during sliding $X_m(\tau)$ satisfies

$$\gamma_m \ddot{X}_m + \theta_m X_m - \eta_m = 0 \quad (2.13)$$

and $X_m(0) = d_m^{k,j}$. The solution of (2.13) is

$$X_m(\tau) = (X_m(0) - \eta_m/\theta_m)\cos\lambda\tau + \eta_m/\theta_m \quad (2.14)$$

The velocity of slip

$$\dot{X}_m(t) = -[X_m(0) - \eta_m/\theta_m]\lambda \sin \lambda t \tag{2.15}$$

will be equal to zero at the time $\tau = \pi/\lambda$ and the final displacement of block m is

$$d_m^{k,j+1} = X_m(\pi/\lambda) = 2\eta_m/\theta_m - X_m(0) = 2\eta_m/\theta_m - d_m^{k,j} \tag{2.16}$$

The relation (2.16) defines the evolution of the model. But we can simplify the expressions if we consider the force f_i applied to the block i instead of the displacement (we assume all quantities are dimensionless)

$$f_i = \theta_i y_i - \sum_{j \neq i} \alpha_{ij} y_j \tag{2.17}$$

Denote $e_m^{k,j}$ the sum of elastic forces applied to the block m from all springs after slip j in event k. Points $\mathbf{e}^{k,j}$ are vertices of a trajectory in the elastic-force phase space. Let $\mu_{i,j} = 2\alpha_{ij}/\theta_i$; then from (2.16) and (2.17) we have in the case of slip of the block m

$$e_m^{k,j+1} = -e_m^{k,j} \tag{2.18}$$

$$e_i^{k,j+1} = e_i^{k,j} + \mu_{m,i} e_m^{k,j} \qquad \text{for} \quad i \neq m \tag{2.19}$$

The failure condition for the block m is

$$f_i \geqslant \beta_i \tag{2.20}$$

In order to describe the evolution of our model, we denote

$$\delta_{i,j} = \min_{k=1,\ldots,N} \frac{\beta_k - e_k^{i,j}}{\alpha_{ii}} \tag{2.21}$$

and the minimum value is on block $m_{i,j}$. Let $e_1^{0,0}, \ldots, e_N^{0,0}$ be the initial elastic forces. If $\delta_{0,0} > 0$, the failure condition is not violated for any block and we have strain accumulation during the time equal to $\delta_{0,0}/v$. Then $e_k^{1,0} = e_k^{0,0} + \alpha_{kk}\delta_{0,0}$, $\delta_{1,0} = 0$, and the elastic force applied to block $m_{1,0} = m_{0,0}$ is $\beta_{m_{1,0}}$. Then block $m_{1,0}$ slips and from (2.18) we have $e_{m_{1,0}}^{1,1} = -e_{m_{1,0}}^{1,0}$ and for $k \neq m_{1,0}$ we have from (2.19) $e_k^{1,1} = e_k^{1,0} + \mu_{m_{1,0}k} e_{m_{1,0}}^{1,0}$. We find $\delta_{1,1}$ and $m_{1,1}$. If $\delta_{1,1} > 0$, the first event is over and we again have a time equal to $\delta_{1,1}/v$ for loading; but if $\delta_{1,1} \leqslant 0$, then block $m_{1,1}$ slips and $e_{m_{1,1}}^{1,2} = -e_{m_{1,1}}^{1,1}$ and for $k \neq m_{1,1}$ we have from (2.19) $e_k^{1,2} = e_k^{1,1} + \mu_{m_{1,1}k} e_{m_{1,1}}^{1,1}$. Block $m_{n,j}$ slides during the $(j+1)$th slip in the nth event and $e_{m_{n,j}}^{n,j+1} = -e_{m_{n,j}}^{n,j}$ and for $k \neq m_{n,j}$ we have $e_k^{n,j+1} = e_k^{n,j} + \mu_{m_{n,j}k} e_{m_{n,j}}^{n,j}$. The nth event ends when $\delta_{n,j} > 0$. So if we denote s_n the number of slips inside of the nth event, we have

$$\mathbf{e}^{0,0} \xrightarrow{\text{loading}} \mathbf{e}^{1,0} \xrightarrow[\text{slip}]{m_{1,0}} \mathbf{e}^{1,1} \xrightarrow[\text{slip}]{m_{1,1}} \cdots \xrightarrow[\text{slip}]{m_{1,s_1-1}}$$

$$\mathbf{e}^{1,s_1} \xrightarrow{\text{loading}} \mathbf{e}^{2,0} \xrightarrow[\text{slip}]{m_{2,0}} \mathbf{e}^{2,1} \xrightarrow[\text{slip}]{m_{2,1}} \cdots \xrightarrow[\text{slip}]{m_{2,s_2-1}} \mathbf{e}^{2,s_2}$$

$$\xrightarrow{\text{loading}} \mathbf{e}^{3,0} \cdots \mathbf{e}^{n,0} \xrightarrow[\text{slip}]{m_{n,0}} \mathbf{e}^{n,1} \xrightarrow[\text{slip}]{m_{n,1}} \cdots \xrightarrow[\text{slip}]{m_{n,s_n-1}} \mathbf{e}^{n,s_n} \cdots$$

We introduce two families of linear maps. $S_m: \mathbf{R}^N \to \mathbf{R}^N$ corresponds to a slip of block m and $L_m: \mathbf{R}^N \to \mathbf{R}^N$ corresponds to a strain accumulation before a slip of block m. We have the map

$$S_m(X_1, \ldots, X_N) = (Y_1, \ldots, Y_n) \tag{2.22}$$

where

$$Y_i = \begin{cases} -X_m, & \text{if } i = m \\ X_i + \mu_{mi} X_m, & \text{otherwise} \end{cases}$$

and the map

$$L_m(X_1, \ldots, X_N) = (X_1 + \beta_m - X_m, \ldots, X_N + \beta_m - X_m) \tag{2.23}$$

Then

$$\mathbf{e}^{n,j+1} = S_{m_{n,j}}(\mathbf{e}^{n,j}); \qquad \mathbf{e}^{n+1,0} = L_{m_{n,s_n}}(\mathbf{e}^{n,s_n}) \tag{2.24}$$

The Jacobian of the map S_m is

$$\mathrm{Jac}(S_m) = \begin{array}{c} \\ 1 \\ 2 \\ \vdots \\ m \\ \vdots \\ N \end{array} \begin{array}{c} \begin{array}{ccccccc} 1 & 2 & \cdots & m & \cdots & N \end{array} \\ \begin{pmatrix} 1 & 0 & \cdots & \mu_{m1} & \cdots & 0 \\ 0 & 1 & \cdots & \mu_{m2} & \cdots & 0 \\ \vdots & \vdots & \ddots & \vdots & \ddots & \vdots \\ 0 & 0 & \cdots & -1 & \cdots & 0 \\ \vdots & \vdots & \ddots & \vdots & \ddots & \vdots \\ 0 & 0 & \cdots & \mu_{mN} & \cdots & 1 \end{pmatrix} \end{array} \tag{2.25}$$

and the Jacobian of the map L_m is

$$\mathrm{Jac}(L_m) = \begin{array}{c} \\ 1 \\ 2 \\ \vdots \\ m \\ \vdots \\ N \end{array} \begin{array}{c} \begin{array}{ccccccc} 1 & 2 & \cdots & m & \cdots & N \end{array} \\ \begin{pmatrix} 1 & 0 & \cdots & -1 & \cdots & 0 \\ 0 & 1 & \cdots & -1 & \cdots & 0 \\ \vdots & \vdots & \ddots & \vdots & \ddots & \vdots \\ 0 & -0 & \cdots & 0 & \cdots & 0 \\ \vdots & \vdots & \ddots & \vdots & \ddots & \vdots \\ 0 & 0 & \cdots & -1 & \cdots & 1 \end{pmatrix} \end{array} \tag{2.26}$$

We now estimate the stability of our system to variations of the initial position. We have a trajectory $\mathbf{e}^{k,j}$ and a variation of the initial position $\mathbf{e}^{0,0'} = \mathbf{e}^{0,0} + \Delta^{0,0}$, where $\Delta^{0,0} \in \mathbf{R}^N$. Denote the difference between the two trajectories $\Delta^{k,j} = \mathbf{e}^{k,j'} - \mathbf{e}^{k,j}$. We take $\Delta^{0,0}$ small enough so that the numbers $m_{k,j}$ are the same for both sequences. Then as S_m and L_m are linear from (2.24) it follows that

$$\Delta^{k,j+1} = S_{m_{k,j}}(\mathbf{e}^{k,j'}) - S_{m_{k,j}}(\mathbf{e}^{k,j}) = \mathrm{Jac}(S_{m_{k,j}})(\Delta^{k,j}) \tag{2.27}$$

and

$$\Delta^{k+1,0} = L_{m_{k,s_k}}(\mathbf{e}^{k,s'_k}) - L_{m_{k,s_k}}(\mathbf{e}^{k,s_k}) = \mathrm{Jac}(L_{m_{k,s_k}})(\Delta^{k,s_k}) \tag{2.28}$$

We denote by $|\mathbf{v}|$ the length of the vector $\mathbf{v} \in \mathbf{R}^N$ and define

$$\Lambda(k,j) = \max_{\Delta^{0,0} \in \mathbf{R}^N} |\Delta^{k,j}|/|\Delta^{0,0}| \tag{2.29}$$

$\Lambda(k,j)$ gives us the maximum possible change of the difference between two close trajectories and

$$\lambda = \lim_{k \to \infty} \lambda_k, \qquad \text{where} \quad \lambda_k = (1/k) \log \Lambda(k,0) \tag{2.30}$$

defines the Lyapunov exponent λ for our model. We apply (2.30) to estimate the stability of different special cases of the general model.

3. TWO-BLOCK MODEL

The simplest example of the general model with $N=2$ is shown in Fig. 2. We will assume symmetry everywhere except for the friction forces. Then $\gamma_1 = \gamma_2 = 1$, $\alpha_{11} = \alpha_{22} = 1$, $\alpha_{12} = \alpha$, $\beta_1 = 1$, $\beta_2 = \beta$; α is a stiffness parameter and the friction parameter β is a measure of the symmetry; the system is symmetric if $\beta = 1$. We have $\theta_1 = \theta_2 = \theta = 1 + \alpha$ and $\mu_{1,2} = 2\alpha/(\alpha+1)$, so the relation between the displacements relative to the driver before and after the slip $(j+1)$ inside sliding event k if it is a slip of block 1 is

$$\begin{aligned} d_1^{k,j+1} &= 2\alpha\, d_2^{k,j}/(1+\alpha) - d_1^{k,j} \\ d_2^{k,j+1} &= d_2^{k,j} \end{aligned} \tag{3.1}$$

If the slip $(j+1)$ inside sliding event k is a slip of block 2, we have

$$\begin{aligned} d_1^{k,j+1} &= d_1^{k,j} \\ d_2^{k,j+1} &= 2\alpha d_1^{k,j}/(1+\alpha) - d_2^{k,j} \end{aligned} \tag{3.2}$$

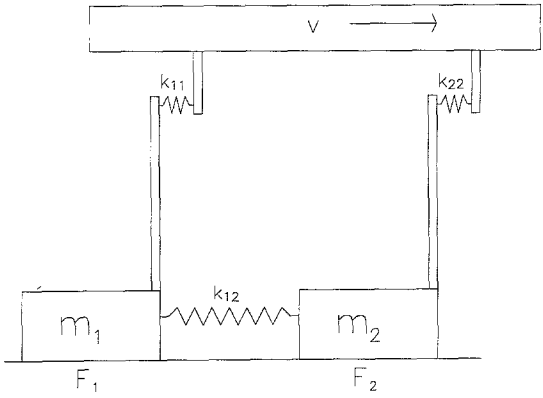

Fig. 2. Illustration of the slider-block model with only two blocks.

The failure criteria are

$$(\alpha+1)d_1^{k,j}-\alpha d_2^{k,j}\geqslant 1 \tag{3.3}$$

$$(\alpha+1)d_2^{k,j}-\alpha d_1^{k,j}\geqslant \beta \tag{3.4}$$

These failure creteria give an area in the displacement phase space which is bordered by two straight lines given by the equalities in (3.3) and (3.4). An example is given in Fig. 3. These straight lines intersect at a point whose location is given by the root of system (2.5) with $N=2$,

$$a_1=\frac{\alpha+1+\alpha\beta}{1+2\alpha} \tag{3.5}$$

$$a_2=\frac{\alpha+\beta+\alpha\beta}{1+2\alpha} \tag{3.6}$$

When $\beta=1$, as in Fig. 3, we have $a_1=a_2=1$. In the triangular region between the straight lines the blocks are stationary; outside this region at least one block violates the failure criteria and will slip.

The expressions (2.18) and (2.19) for forces when block 1 slides are

$$\begin{aligned} e_1^{k,j+1} &= -e_1^{k,j} \\ e_2^{k,j+1} &= e_2^{k,j}+[2\alpha/(\alpha+1)]e_1^{k,j} \end{aligned} \tag{3.7}$$

and when block 2 slides they are

$$\begin{aligned} e_1^{k,j+1} &= e_1^{k,j}+[2\alpha/(\alpha+1)]e_2^{k,j} \\ e_2^{k,j+1} &= -e_2^{k,j} \end{aligned} \tag{3.8}$$

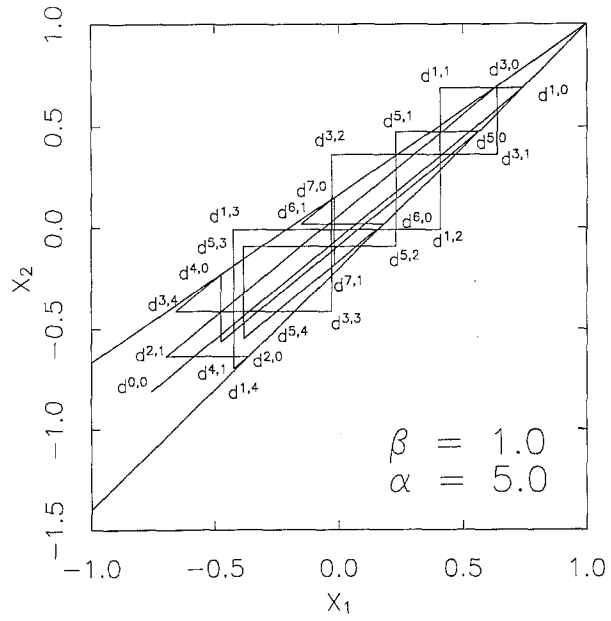

Fig. 3. Phase portrait of the evolution into a periodic trajectory with $\alpha = 5$ and $\beta = 1$. The diagonal lines converginig on $X_2 = X_1 = 1$ in the X_2–X_1 phase plane are the failure envelope given by (3.3) and (3.4). The trajectory begins with displacement $d^{0,0}$ and evolves to the periodic trajectory $d^{6,0} \to d^{6,1} \to d^{7,0} \to d^{7,1} \to d^{6,0}$.

The failure criteria are

$$e_1^{k,j} \geqslant 1; \qquad e_2^{k,j} \geqslant \beta \tag{3.9}$$

For $N = 2$ we can write simple expressions for the dependence of the forces after slip j inside sliding event k, $\mathbf{e}^{k,j}$, on the forces before sliding event k, $\mathbf{e}^{k,0}$. Let ϑ be a real number such that $0 < \vartheta < \pi/2$ and $\cos\vartheta = \alpha/(\alpha+1)$. Denote

$$G_{\beta,n}(x, \vartheta) = [x \sin n\vartheta + \beta \sin(n+1)\vartheta]/\sin\vartheta \tag{3.10}$$

Then if the first slip in the event k is the slip of block 1, we have $e_1^{k,0} = 1$ and for even j

$$e_1^{k,j} = G_{1,j}(e_2^{k,0}, \vartheta) \tag{3.11}$$

$$e_2^{k,j} = -G_{1,j-1}(e_2^{k,0}, \vartheta) \tag{3.12}$$

and for odd j

$$e_1^{k,j} = -G_{1,j-1}(e_2^{k,0}, \vartheta) \tag{3.13}$$

$$e_2^{k,j} = G_{1,j}(e_2^{k,0}, \vartheta) \tag{3.14}$$

If the first slip in the event k is the slip of block 2, we have $e_2^{k,0} = \beta$ and for odd j

$$e_1^{k,j} = G_{\beta,j}(e_2^{k,0}, \vartheta) \tag{3.15}$$

$$e_2^{k,j} = -G_{\beta,j-1}(e_2^{k,0}, \vartheta) \tag{3.16}$$

and for even j

$$e_1^{k,j} = -G_{\beta,j-1}(e_2^{k,0}, \vartheta) \tag{3.17}$$

$$e_2^{k,j} = G_{\beta,j}(e_2^{k,0}, \vartheta) \tag{3.18}$$

Expressions (3.11)–(3.18) can be proven using mathematical induction.

Let m be the integer part of π/ϑ ($m > 1$ as $\vartheta < \pi/2$); then

$$\begin{aligned} &\sin(m-1)\vartheta > 0; \qquad \sin m\vartheta > 0 \\ &\sin(m+1)\vartheta < 0; \qquad \sin(m+2)\vartheta < 0 \end{aligned} \tag{3.19}$$

Thus from (3.11)–(3.18) it follows that the maximum number of slips inside a sliding event is not more than $m+1$, so that we always have a finite number of slips inside the sliding event. If we assume that we do not have less than $m+2$ slips inside a sliding event, we have from (3.9) and (3.11)–(3.18) that $G_{\beta,j+1}(e_2^{k,0}, \vartheta) \geqslant 1$ and $G_{\beta,j}(e_2^{k,0}, \vartheta) \geqslant 1$ (they sometimes should be $\geqslant \beta$). But it follows from (3.19) that $G_{\beta,j+1}(e_2^{k,0}, \vartheta) < 0$ for positive $e_2^{k,0}$ and $G_{\beta,j}(e_2^{k,0}, \vartheta) < 0$ for negative $e_2^{k,0}$, so we have a contradiction.

A typical phase portrait for a symmetrical example is given in Fig. 3 with $\alpha = 5$ and $\beta = 1$. The sequence of slip events begins with the initial displacement $d^{0,0}$. Both blocks stick and we have strain accumulation to point $d^{1,0}$, where the failure criterion (3.3) for block 1 is violated. Block 1 slides and stops at point $d^{1,1}$, but this point satisfies the failure criterion for block 2, (3.4), and it begins to slide. Block 2 stops at point $d^{1,2}$, but this point again violates the failure criterion for block 1. Block 1 slides and stops at point $d^{1,3}$, where the failure criterion for block 2 is violated and block 2 slides to point $d^{1,4}$. We then have a period of strain accumulation $d^{1,4}d^{2,0}$. We next have a single-slip event $d^{2,0}d^{2,1}$ with a slip of block 1. After loading $d^{2,1}d^{3,0}$ we have a multiple-slip event which is started by block 2. We have two slips of block 2: $d^{3,0}d^{3,1}$ and $d^{3,2}d^{3,3}$; and two slips of block 1: $d^{3,1}d^{3,2}$ and $d^{3,3}d^{3,4}$. After the strain accumulation $d^{3,4}d^{4,0}$ we have a single block 2 slip $d^{4,0}d^{4,1}$. After loading $d^{4,1}d^{5,0}$ we again have a multiple-slip event consisting of two slips of block 1: $d^{5,0}d^{5,1}$ and $d^{5,2}d^{5,3}$; and two slips of block 2: $d^{5,1}d^{5,2}$ and $d^{5,3}d^{5,4}$. After the strain accumulation $d^{5,4}d^{6,0}$ we have a single slip of block 1, $d^{6,0}d^{6,1}$; then loading $d^{6,1}d^{7,0}$

and a single slip of block 2, $d^{7,0}d^{7,1}$. But after the strain accumulation we come to the same point $d^{6,0}$ and the last two events will repeat indefinitely. After an interval of rather complicated evolution we come to a periodic trajectory which consists only of single-slip events.

It is also instructive to illustrate the behavior of the system using a Poincaré map. For this purpose we will consider only sliding events (including multiple events) that begin with the slip of the first block. The nondimensional force $e_1^{k,0}$ applied to the first block when it initially slips is always equal to 1. So we take all k_j such that $e_1^{k_j,0} = 1$. The behavior of the system can be characterized by the sequence of nondimensional forces applied to the second block $f_j = e_2^{k_j,0}$ when the slip of the first block begins. Since the second block must be at or below the slip condition, we have $f_j \leqslant \beta$. This sequence of values f_j defines a Poincaré function and the iteration of this function determines the evolution of the system.

We first consider the Poincaré map for $\alpha = 5$ and $\beta = 1$; it is given in Fig. 4. The dependence of f_{j+1} on f_j is a rather complicated piecewise linear function. Also included in Fig. 4 is the diagonal line $f_{j+1} = f_j$. Intersections of the Poincaré map with the diagonal line are the fixed points of the solution. It is seen that there are four unstable fixed points at

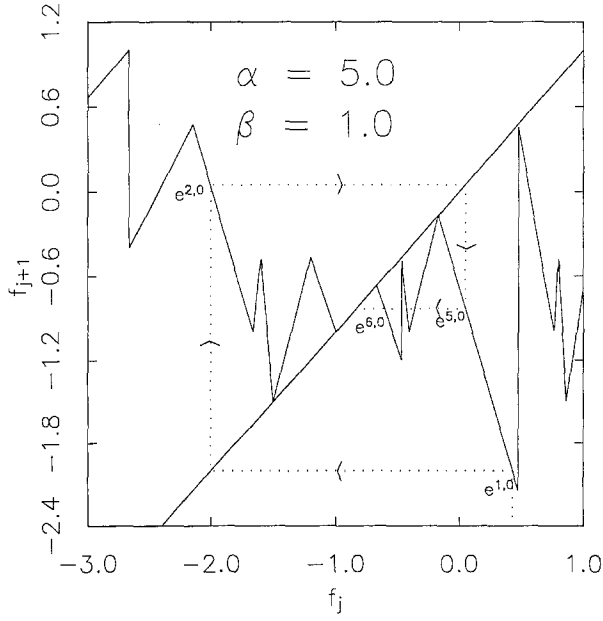

Fig. 4. Poincaré map for $\alpha = 5$ and $\beta = 1$. The sequence of dimensionless forces f_i applied to the second block when slip of the first block begins is given. The dotted line illustrates the phase trajectory given in Fig. 3.

$f_{j+1}=f_j=-1.5$, -0.5, -0.17, and 0.48; there is also an infinite set of fixed points in the range $-1<f_{j+1}=f_j<-0.6667$; these are stable fixed points. The fixed point that the solution approaches in the steady state depends upon the initial values of the iteration. The same example which is shown in Fig. 3 in displacement phase space is given in Fig. 4 in the Poincaré map. The initial force is $e_2^{1,0}=0.43$. Then $e_2^{2,0}=-2$, and the next point is $e_2^{5,0}=-0.05$. We skip $e^{3,0}$ and $e^{4,0}$, as events 3 and 4 started from the slip of block 2, and for them $e_2^{3,0}<1$ and $e_1^{4,0}<1$. The last point $e^{6,0}$ is in the infinite set of fixed points and from this point a periodic trajectory starts.

For the symmetric case $\beta=1$ we always have an infinite set of fixed points over the range $-1<f_{j+1}=f_j<1-2\alpha/(\alpha+1)$. If $-1<f_j=e_2^{k,0}<1-2\alpha/(\alpha+1)$ and $e_1^{k,0}=1$, block 1 slides and using (3.7) we have $e_1^{k,1}=-1$ and

$$-1+2\alpha/(\alpha+1)<e_2^{k,1}=e_2^{k,0}+2\alpha/(\alpha+1)<1 \tag{3.20}$$

The failure criteria are not violated and we have loading until $e_2^{k+1,0}=1$. Then $-1<e_1^{k+1,0}=-e_2^{k,1}<1-2\alpha/(\alpha+1)<1$. Block 2 slides and after it stops, from (3.8), we have $e_2^{k+1,1}=-1$ and $e_1^{k+1,1}=e_1^{k+1,0}+2\alpha/(\alpha+1)$. Thus $-1+2\alpha/(\alpha+1)<e_1^{k+1,1}<1$ and again the failure criteria are not violated and we have the strain accumulation until $e_1^{k+2,0}=1$ and from (3.20) it follows that

$$\begin{aligned} f_{j+1}=e_2^{k+2,0}&=-e_1^{k+1,1}=-e_1^{k+1,0}-2\alpha/(\alpha+1)\\ &=e_2^{k,1}-2\alpha/(\alpha+1)=e_1^{k,0}=f_j \end{aligned}$$

Thus we have periodic trajectories over the whole interval of fixed points. Note that for all the linear segments of the Poincaré map we have $df_{j+1}/df_j\geqslant 1$, so that if our initial condition f_0 lies outside the interval of fixed points, there will be a transient iteration before the trajectory lands on the interval of fixed points. The length of the fixed point interval decreases and the length of the transient increases with increasing α. For the symmetric case we always have a periodic trajectory in the steady state, but the trajectory depends upon the initial conditions.

The Poincaré map for $\alpha=0.2$ and $\beta=3$ is given in Fig. 5. In general it can be shown that

$$f_{j+1}=f_j+2+2\cos\theta \tag{3.21}$$

for $f_j\leqslant\beta-2-2\cos\theta$. If $f_j=e_2^{k,0}$ after the slip of block 1 we have

$$e_1^{k,1}=-1; \qquad e_2^{k,1}=e_2^{k,0}+2\cos\theta \tag{3.22}$$

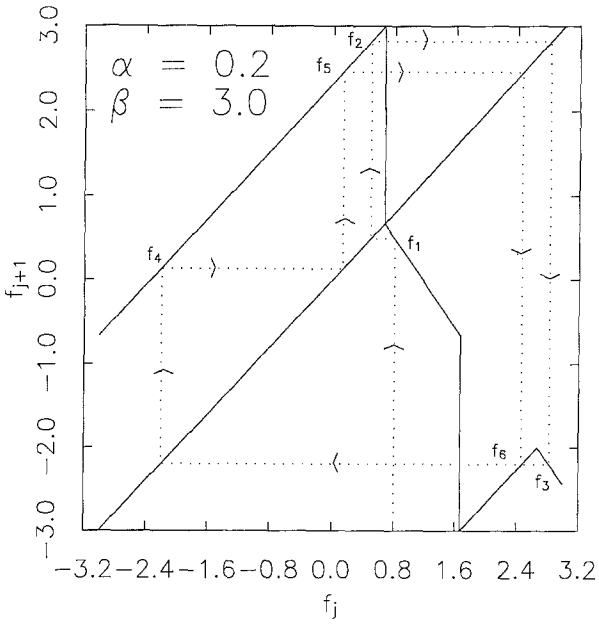

Fig. 5. Poincaré map for $\alpha = 0.2$ and $\beta = 3$. The dotted line illustrates the evolution of a trajectory from the initial value $f_0 = 0.8$ to the periodic trajectory $f_4 \to f_5 \to f_6 \to f_4$.

Thus $e_2^{k,1} < \beta - 2$ and we have strain accumulation until both forces increase by 2 and $e_1^{k+1,0} = 1$ and $f_{j+1} = e_2^{k+1,0} = e_2^{k,0} + 2 + 2\cos\theta < \beta$, so (3.21) is true. As a result, the Poincaré map in Fig. 5 has unit slope for $e_{2n} \leqslant 2/3$.

If can also be shown that

$$f_{j+1} = f_j - (\beta - 1)(2 + 2\cos\theta) \tag{3.23}$$

for $\beta - 2\cos\theta - 2 + 2\beta\cos\theta < f_j < \beta - 2\cos\theta$. There exists f_j which satisfies this inequality if, as in our case, $\beta < 1 + 1/\alpha$. After the slip of block 1 we again have (3.22) and $\beta - 2 + 2\beta\cos\theta < e_2^{k,1} < \beta$, but now the next event starts from block 2 because $2 - 2\beta\cos\theta < 2$. So we have $e_2^{k+1,0} = \beta$ and $e_1^{k+1,0} = -1 + \beta - f_j - 2\cos\theta < 1$. After the slip of block 2 we have $e_2^{k+1,1} = -\beta$ and $e_1^{k+1,1} = -1 + \beta - f_j - 2\cos\theta + 2\beta\cos\theta$. The next event starts from the slip of block 1, so $e_1^{k+2,0} = 1$ and $e_2^{k+2,0} = -\beta + 1 - e_1^{k+1,1}$, which gives us (3.23). So if $\beta < 1 + 1/\alpha$ is an integer, we always have a periodic trajectory which starts from (3.23) and then (3.21) repeats $\beta - 1$ times and again we have the whole interval of initial positions, which gives us a periodic trajectory.

As a specific example, we take $f_0 = e_2^{0,0} = 0.8$ and the resulting iterations are given by the dotted line in Fig. 5. We obtain the sequence of points f_i with

$$f_1 = 0.49 \to f_2 = 2.82 \to f_3 = -2.2 \to f_4 = 0.13 \to f_5 = 2.46 \to f_6 = -2.2$$

We see that points f_4, f_5, and f_6 form a periodic trajectory. The corresponding periodic trajectory phase portrait is shown in Fig. 6. Points $d_{4,0}$, $d_{5,0}$, and $d_{6,0}$ in Fig. 6 correspond to the points f_4, f_5, and f_6 in Fig. 5. The periodic trajectory starts from the point $d^{4,0}$ when block 1 slides and then stops at the point $d^{4,1}$. Then we have loading to the point $d^{5,0}$, where again the first block begins to slide. Its slip terminates at $d^{5,1}$ and again we have loading until the point $d^{6,0}$. Again block 1 slides and stops at $d^{6,1}$. Then we have loading and now block 2 slides at the point $d^{7,0}$. The second block stops at $d^{7,1}$ and after loading we return to the initial point $d^{4,0}$. Note that (3.21) is applicable twice and (3.23) once in our periodic trajectory. If $5/3 \leqslant f_j \leqslant 8/3$, we always have periodic trajectories, so that again we have a cyclic evolution in the steady state and the trajectory depends upon the initial conditions.

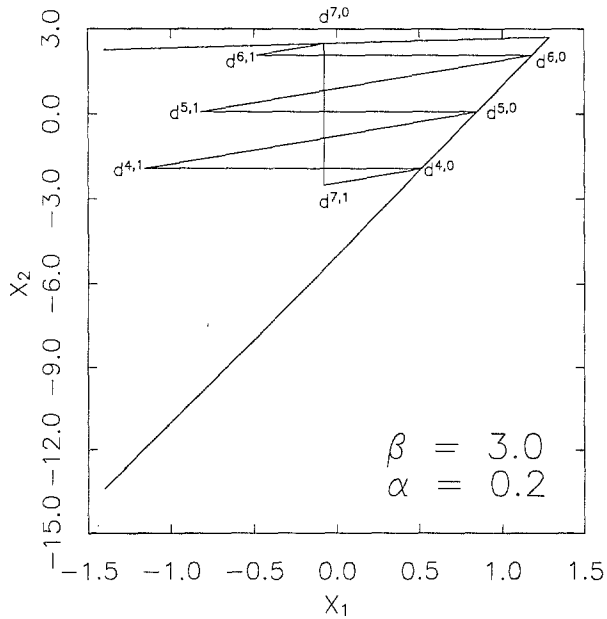

Fig. 6. Phase portrait of the periodic trajectory for $\alpha = 0.2$ and $\beta = 3$ corresponding to the evolution from $f_0 = 0.8$ given in Fig. 5.

We next consider the case in which the strengths of the driver and coupling springs are equal, $\alpha = 1$ and $2\cos\theta = 1$. For this case we can show that $f_{j+1} = f_j$ in the range $\beta - 1 < f_j < \beta$ if $\beta \geqslant 2$ and that $f_{j+1} = f_j$ in the range $1 < f_j < \beta$ if $\beta < 2$. Again $e_1^{k,0} = 1$ and $f_j = e_2^{k,0} < \beta$. After the slip of block 1 we have $e_1^{k,1} = -1$ and $e_2^{k,1} = f_j + 1 > \beta$. Now block 2 slips and $e_1^{k,2} = -1 + 1 + f_j > 1$ and $e_2^{k,2} = -f_j - 1$. The failure criterion for block 1 is satisfied and after it slips $e_1^{k,3} = -f_j$ and $e_2^{k,3} = -1$. The next event starts from block 1 and $e_1^{k+1,0} = 1$ and $f_{j+1} = e_2^{k+1,0} = 1 - e_1^{k,3} = f_j < \beta$. Again we have an interval of fixed points. The Poincaré map for $\alpha = 1$ and $\beta = 1.3$ is given in Fig. 7. We see that $f_{j+1} = f_j$ in the interval $1 < f_j < 1.3$. In this range of initial conditions we have periodic trajectories that depend on the initial conditions; an example with $f_0 = 1.1$ is given in Fig. 8. The periodic trajectory starts from point $d^{0,0}$ where block 1 slides and stops at point $d^{0,1}$, but this point satisfies the failure criterion for block 2 and it begins to slide. Block 2 stops at point $d^{0,2}$, but this point satisfies the failure criterion for block 1 and it begins to slide. The multiple-slip episode terminates at point $d^{0,3}$ and we have loading that returns us to point $d^{0,0}$.

We next consider the interval I of values for f_j illustrated in Fig. 7. If f_j is within this interval, then the point f_{j+1} must also lie within this interval. Because the slopes of the Poincaré map within this region are

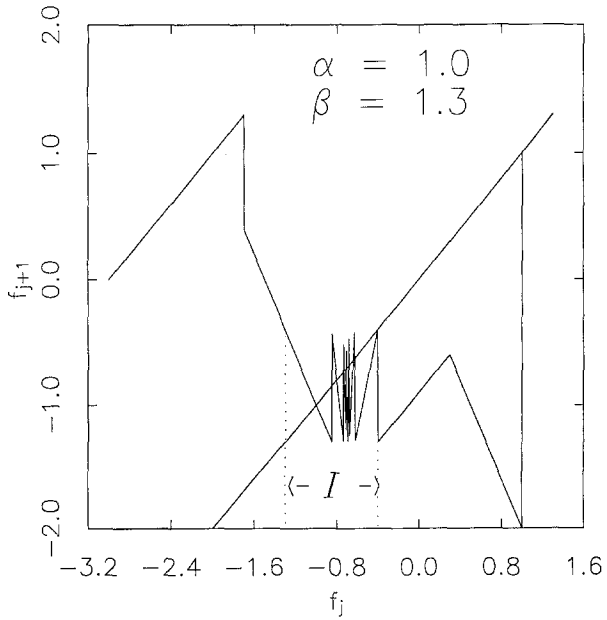

Fig. 7. Poincaré map for $\alpha = 1$ and $\beta = 1.3$. Orbits within the interval I are trapped and the resulting phase portraits are chaotic; an example is given in Fig. 9.

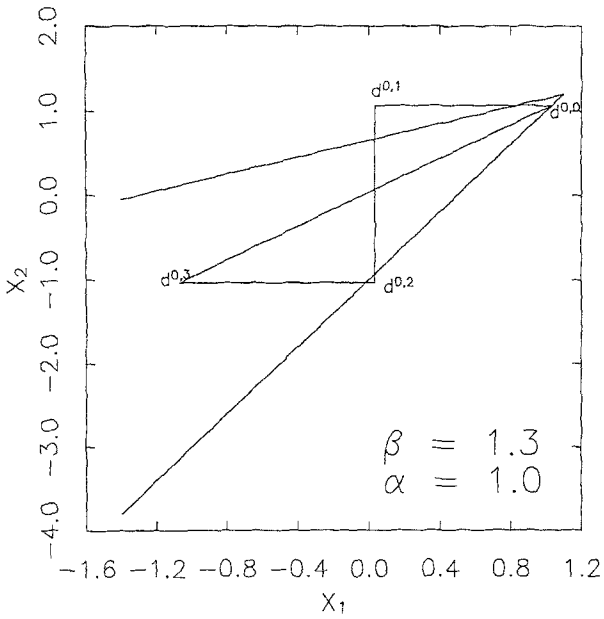

Fig. 8. Phase portrait of a periodic trajectory with $\alpha = 1$, $\beta = 1.3$, and $f_0 = 1.1$.

greater than unity, the singular points are unstable and we expect chaotic behavior. An example with $f_0 = -0.8$ is given in Fig. 9. For the parameter values $\alpha = 1$ and $\beta = 1.3$ we have either chaotic behavior or periodic behavior, depending upon the initial conditions.

We next illustrate an example in which the solution asymptotically approaches a limit cycle trajectory. The Poincaré map for $\alpha = 3.5$ and $\beta = 3$ is given in Fig. 10. We first consider initial values in the interval $2.15 < f_0 < 3$ ($f_0 = 3$ is the maximum allowed value for $\beta = 3$); we denote this interval as $a_0 b_0$ in Fig. 10. After the first iteration we have $-0.15 < f_1 < 0.06$ corresponding to the interval $a_1 b_1$ and after the second iteration we have $2.54 < f_2 < 2.98$ corresponding to the interval $a_2 b_2$. Thus, after each two iterations the length of interval becomes less and asymptotically we will have a point instead of the interval. The asymptotic cyclic trajectory is shown in Fig. 10 as the dotted line. It oscillates between the points $e^{0,0}$ with $f_0 = 2.7$ and $e^{1,0}$ with $f_1 = -0.013$. Note that $f_2 = f_0$ and we have a period-two limit cycle. For any other initial conditions the trajectory will enter this region and will converge to the limit cycle. The limit cycle behavior in the phase plane is illustrated in Fig. 11. The failure of block 1 at point $d^{0,0}$ in the phase portrait corresponds to point $e^{0,0}$ in the Poincaré map. This is a multiple failure with three failures of block 1,

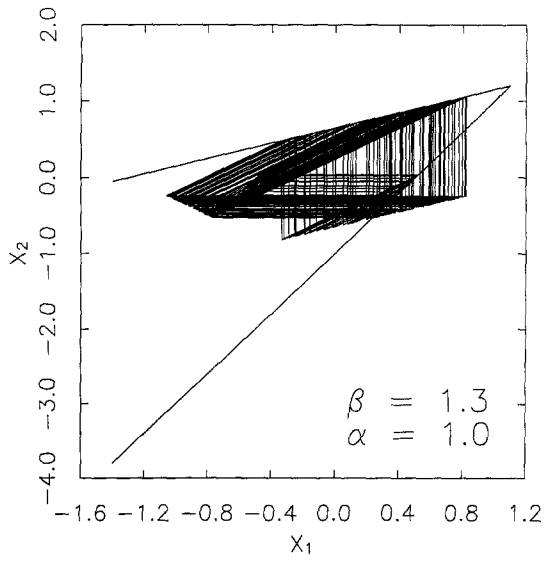

Fig. 9. Phase portrait of a chaotic trajectory with $\alpha = 1$, $\beta = 1.3$, and $f_0 = -0.8$.

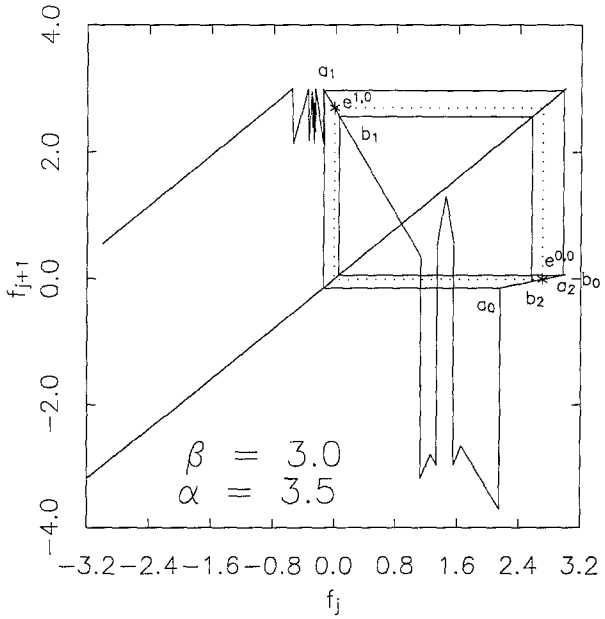

Fig. 10. Poincaré map for $\alpha = 3.5$ and $\beta = 3$. The dotted line corresponds to the period-two limit cycle illustrated in Fig. 11. Trajectories for all initial values f_0 converge to this limit cycle.

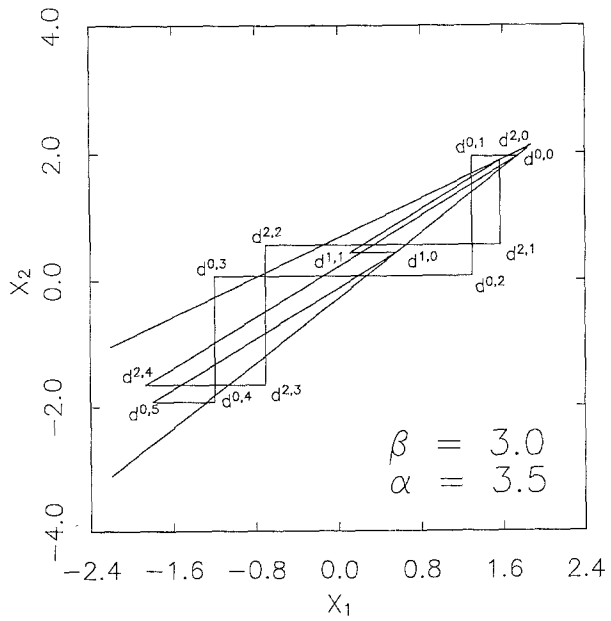

Fig. 11. Phase portrait of a period-two limit cycle for $\alpha = 3.5$ and $\beta = 3$. Trajectories for all initial conditions converge on this limit cycle.

$d^{0,0}d^{0,1}$, $d^{0,2}d^{0,3}$, and $d^{0,4}d^{0,5}$, and two failures of block 2, $d^{0,1}d^{0,2}$ and $d^{0,3}d^{0,4}$. After strain accumulation $d^{0,5}d^{1,0}$, block 1 fails, $d^{1,0}d^{1,1}$, and this corresponds to $e^{1,0}$ on the Poincaré map. After strain accumulation $d^{1,1}d^{2,0}$, block 2 fails. This is a multiple failure with two failures of block 2, $d^{2,0}d^{2,1}$ and $d^{2,2}d^{2,3}$, and two failures of block 1, $d^{2,1}d^{2,2}$ and $d^{2,3}d^{2,4}$. After strain accumulation $d^{2,4}d^{0,0}$ the period-two limit cycle repeats.

Our last example is for $\alpha = 2$ and $\beta = 3$. The Poincaré map for these parameter values is given in Fig. 12 and a phase portrait for $f_0 = 0.1$ is given in Fig. 13. The behavior in this case is clearly chaotic. With asymmetry the system exhibits a great variety of behavior. For the last example the trajectories are chaotic for all initial conditions. We have also illustrated examples in which the behavior is chaotic for some initial conditions and evolves into periodic orbits for other initial conditions and limit-cycle behavior that is independent of initial conditions.

We next determine the Lyapunov exponent for several cases. We can define the Lyapunov exponent λ not only from (2.30), but also using the Poincaré map

$$\lambda = \lim_{k \to \infty} \frac{1}{k} \sum_{j=1}^{k} \log \left| \frac{df_{j+1}}{df_j} \right| \tag{3.24}$$

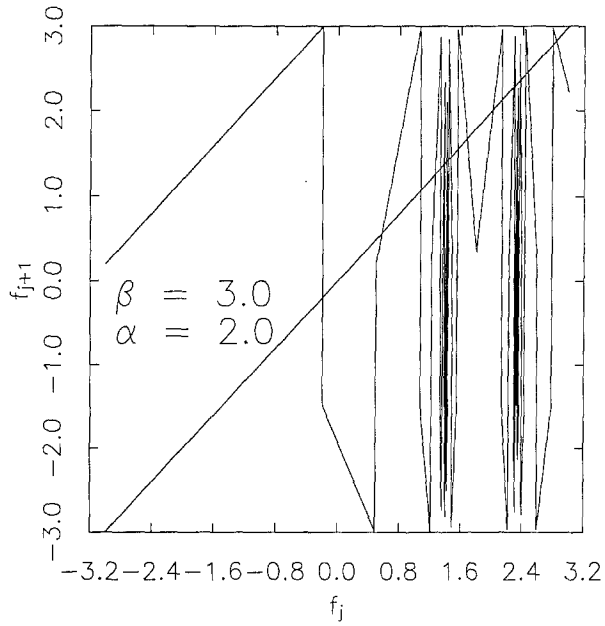

Fig. 12. Poincaré map for $\alpha = 2$ and $\beta = 3$.

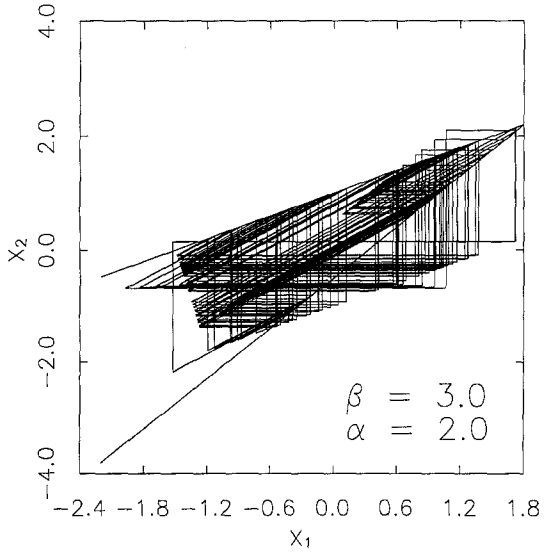

Fig. 13. Phase portrait of a chaotic trajectory with $\alpha = 2$, $\beta = 3$, and $f_0 = 0.1$.

for any trajectory. In the case $\alpha = 2$ and $\beta = 3$ we have $|df_{j+1}/df_j| \geqslant 2$ for $f_j > -1/3$. We will prove this by using the fact that a force on a block before an event is a linear function of the force before the previous event and so the dependence of f_{j+1} on f_j is the composition of the linear functions and $|df_{j+1}/df_j|$ is equal to a product of derivatives of these functions. With $e_2^{k,0} = f_j > -1/3$, let l be a number such that event l is the next after event k which starts from block 1. Then $f_{j+1} = e_2^{l,0}$; $e_1^{k,0} = e_1^{l,0} = 1$. Note that $e_2^{k,1} = f_j + 4/3 > 1$. We consider two cases:

1. $f_j < 5/3$. Then $e_2^{k,1} < 3$ and the $(k+1)$ event starts from block 2; $e_1^{k+1,0}$ is a linear function of f_j, $e_1^{k+1,0} = 2/3 - f_j = a_k f_j + b_k < 1$ and $l > k$. Note that in this case $|a_k| = 1$, but $e_1^{k+1,0} > -1$.
2. $f_j \geqslant 5/3$. Then $e_2^{k,1} \geqslant 3$ and block 2 slides. Then $e_2^{k,2} = -f_j - 4/3$ and $e_1^{k,2} = (4/3) f_j + 7/9 > 1$; so now block 1 slides and $e_1^{k,3} = (-4/3) f_j - 7/9 < -19/9$; $e_2^{k,3} = (7/9) f_j - 8/27 < 3$. Now the sliding event is over and the next event starts from block 2 and $e_1^{k+1,0} = (-19/9) f_j + 68/27 < 1$. Thus in this case also $l > k$ and $e_1^{k+1,0} = a_k f_j + b_k$ with $|a_k| \geqslant 2$.

Let $k < m < l$; then $e_2^{m,0} = 3$ and $e_1^{m,0} < 1$, as event m starts from block 2. We now prove that for $m < l - 1$ we have $e_1^{m+1,0} = a_m e_1^{m,0} + b_m$ and for $m = l - 1$ we have $e_2^{l,0} = a_m e_1^{m,0} + b_m$ with $|a_m| \geqslant 1$. For $f_j < 5/3$ when $|a_k| = 1$ we have $|a_{k+1}| \geqslant 2$ and for $f_j \geqslant 5/3$ we have $|a_k| \geqslant 2$, so that

$$\left| \frac{df_{j+1}}{df_j} \right| = \prod_{i=k}^{l-1} |a_i| \geqslant 2 \tag{3.25}$$

because in the product all terms are not less than 1 and at least one term is greater than 2. We have $e_1^{m,1} = e_1^{m,0} + 4$ and $e_2^{m,1} = -3$. Now we have two different cases:

1. $e_1^{m,0} < -3$. When event m is over, for $m < l - 1$ we have $e_1^{m+1,0} = 10 + e_1^{m,0}$; for $m = l - 1$ we have $e_2^{m+1,0} = -6 - e_1^{m,0}$; in any case $|a_m| = 1$, but this situation is possible only for $f_j \geqslant 5/3$.
2. $e_1^{m,0} \geqslant -3$ (this is the case for $f_j < 5/3$). Then block 1 slides and $e_1^{m,1} = -4 - e_1^{m,0}$; $e_2^{m,1} = (4/3) e_1^{m,0} + 7/3$. And again we have two different cases.

   2.1. $e_2^{m,1} < 3$. When event m is over, for $m < l - 1$ we have $e_1^{m+1,0} = (-7/3) e_1^{m,0} - 10/3$ and for $m = l - 1$ we have $e_2^{m+1,0} = (7/3) e_1^{m,0} + 22/3$, so in any case $|a_m| > 2$.

   2.2. $e_2^{m,1} \geqslant 3$. When block 2 slides, $e_1^{m,2} = (7/9) e_1^{m,0} - 8/9 < 1$; $e_2^{m,2} = (-4/3) e_1^{m,0} - 7/3 < 0$. Thus now event m is over and for

$m < l-1$ we have $e_1^{m+1,0} = (19/9)e_1^{m,0} + 40/9$ and for $m = l-1$ we have $e_2^{m+1,0} = (-19/9)e_1^{m,0} - 4/9$, so again in any case $|a_m| > 2$ and (55) is proven.

Note that $|f_{j+1}| < (1+3)/\sin\vartheta = 12/\sqrt{5} < 6$ for any $f_j > -1/3$, because in (3.11)–(3.18) $x < 1$ and $\beta < 3$ or $x < 3$ or $\beta < 1$. Thus $f_{j+1} > -6$ and if $f_{j+1} < -1/3$ and $f_{j+2} = f_{j+1} + 10/3 < -1/3$, then $f_{j+2} = f_{j+1} + 20/3 > -1/3$, so at least 1/3 of all terms in the sum on the right side of (3.24) are not less than $\log 2$ and other terms are nonnegative:

$$\frac{1}{k}\sum_{j=1}^{k} \log\left|\frac{df_{j+1}}{df_j}\right| \geqslant \frac{1}{3}\log 2$$

Thus, $\lambda \geqslant \frac{1}{3}\log 2$ for $\alpha = 2$ and $\beta = 3$ and we have a positive Lyapunov exponent in this case.

We now apply (2.30) to our two-block model and determine what this technique gives us in a case when we know that the Lyapunov exponent is positive. We have from (2.25) and (2.26)

$$\begin{aligned} \mathrm{Jac}(S_1) &= \begin{pmatrix} -1 & 0 \\ \frac{4}{3} & 1 \end{pmatrix}; \qquad \mathrm{Jac}(S_2) = \begin{pmatrix} 1 & \frac{4}{3} \\ 0 & -1 \end{pmatrix} \\ \mathrm{Jac}(L_1) &= \begin{pmatrix} 0 & 0 \\ -1 & 1 \end{pmatrix}; \qquad \mathrm{Jac}(L_2) = \begin{pmatrix} 1 & -1 \\ 0 & 0 \end{pmatrix} \end{aligned} \tag{3.26}$$

And from (2.30), $\lambda = \lim_{k\to\infty} \lambda_k$, where

$$\lambda_k = (1/k)\log \Lambda(k,0) = (1/k)\log \max_{\Delta^{0,0}\in \mathbf{R}^2} |\Delta^{k,0}|/|\Delta^{0,0}| \tag{3.27}$$

In the case of the two-block model we could use (3.27), but in the two-dimensional case it is very difficult to find a maximum. We will not take the maximum in (3.27), but we use

$$\Lambda(k,j) = |\Delta^{k,j}|/|\Delta^{0,0}| \tag{3.28}$$

For arbitrary $|\Delta^{0,0}|$ this gives us a lower estimate for λ_k. The dependence of $\lambda_k = (1/k)\log \Lambda(k,0)$ on k is given in Fig. 14 for the periodic case $\alpha = 20$ and $\beta = 1$ and in Fig. 15 for the chaotic case $\alpha = 2$ and $\beta = 3$. We can see that in the periodic case we have positive values of λ_k until the system enters the periodic trajectory and then λ_k tends to 0, so that $\lambda = 0$. In the chaotic case the Lyapunov exponent is $\lambda = 0.45$ and is positive as expected.

It is of interest to discuss whether the restriction that only one block slips at once has a major influence on the behavior of the dynamical system. This restriction allows us to reduce the problem to a solution valid

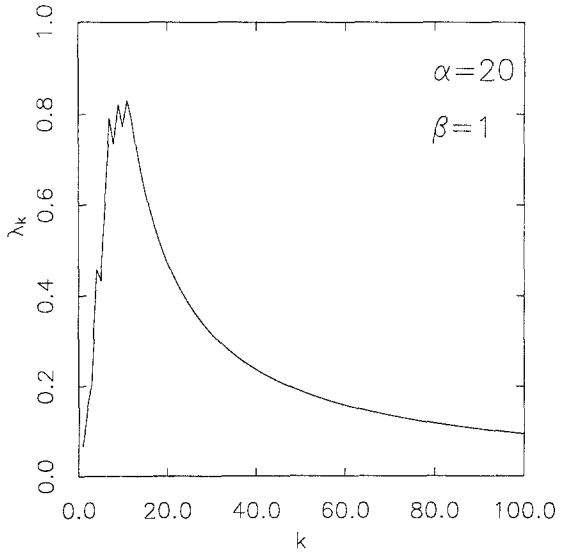

Fig. 14. The Lyapunov exponent λ is defined by the relation $\lambda = \lim_{k \to \infty} \lambda_k$. The dependence of λ_k on k is given for $\alpha = 20$ and $\beta = 1$.

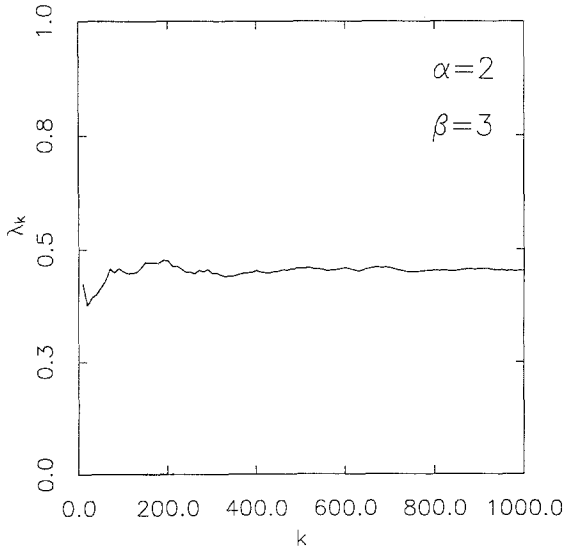

Fig. 15. The dependence of λ_k on k is given for $\alpha = 2$ and $\beta = 3$.

for any value of the dynamic friction, including no dynamic friction, in which case no energy is dissipated. The results obtained here are very similar to those obtained by Huang and Turcotte[4] in which both blocks were allowed to slide at once. In both cases choatic behavior is found for a range of parameter values.

4. TWO-DIMENSIONAL MODEL

We will next apply our model to the behavior of large arrays of slider blocks. We consider rectangular arrays made up of $N = n \cdot m$ blocks; the numbering of the blocks is illustrated in Fig. 16. All blocks are connected to a constant-velocity driver and to adjacent blocks by springs; the blocks are constrained to move only in the x direction. We assume complete symmetry and take $\gamma_i = 1$, $\alpha_{ii} = 1$, $\beta_i = 1$, and $\alpha_{ij} = \alpha$ for neighboring blocks i and j and $\alpha_{ij} = 0$ in other cases. This model is essentially a cellular automaton. A slip occurs when the failure criterion (2.3) is violated. The failure of the first block may transfer sufficient force to the adjacent blocks, through the connector springs, to cause one or more of these blocks to fail.

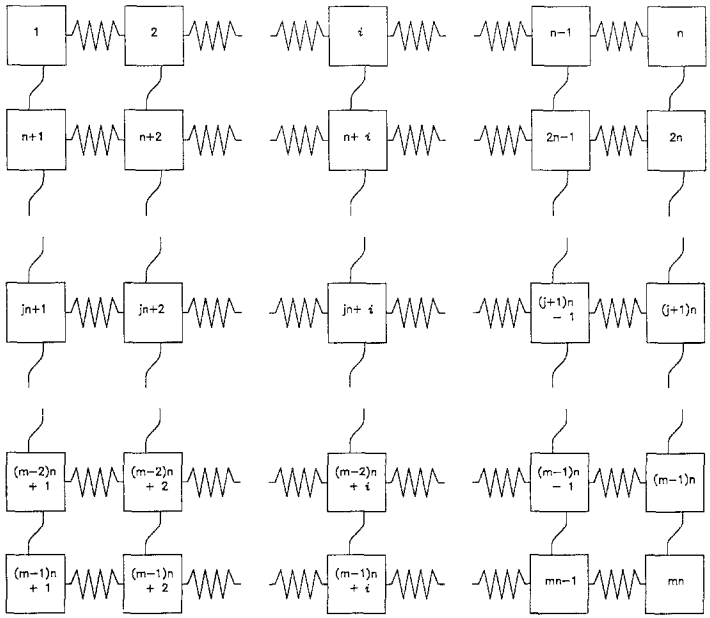

Fig. 16. Illustration of a two-dimensional $n \times m$ array of slider blocks. All blocks are connected to a constant driver and to adjacent blocks by springs; the blocks are constrained to move in the x direction.

All blocks for which the failure condition is violated are allowed to fail sequentially. The sequence is arbitrary but the evolution of the system is not sensitive to the choice.

The boundary conditions on the sides of the array are taken to be either free or periodic. Most of our studies have utilized free surface boundary conbditions. For free surface boundary conditions, $\theta_i = 1 + 4\alpha$ if the block is not on the boundary (if $i = kn + r$ with integer k and r and $0 \leqslant r < n$, then r should not be equal to 0 or 1); $\theta_i = 1 + 2\alpha$ if the block is in the corner $[i = 1;\ i = n;\ i = (m-1)n + 1;\ i = mn]$; $\theta_{i,j} = 1 + 3\alpha$ in other cases and $\mu_{i,j} = 2\alpha/\theta_i$ for neighboring blocks i and j and $\mu_{i,j} = 0$ in other cases.

We now define the evolution of the model. Let $e_i^{k,j}$ be the force on block i after the slip j in event k and $m_{k,j}$ be the number of the block which slides during slip $j+1$ in event k, i.e., $e_{m_{k,j}}^{k,j} = \max_{i=1,\ldots,N} e_i^{k,j}$. Then

$$e_i^{k,j} = \begin{cases} -e_i^{k,j-1} & \text{if } \ i = m_{k,j-1} \\ e_i^{k,j-1} + 2\alpha/\theta_m e_{m_{k,j-1}}^{k,j-1} & \text{if blocks } i \text{ and } m_{k,j-1} \\ & \text{are neighbors} \\ e_i^{k,j-1} & \text{otherwise} \end{cases} \tag{4.1}$$

If

$$e_{m_{k,j}}^{k,j} \geqslant 1 \tag{4.2}$$

then block $m_{k,j}$ slides. If (4.2) is not true, the sliding event is over and we have uniform loading until the failure criterion is again violated. Denote $\delta_{k,j} = \min_{i=1,\ldots,N} 1 - e_i^{k,j} = 1 - e_{m_{k,j}}^{k,j}$. If the failure criteria are not violated,

$$e_i^{k+1,0} = e_i^{k,j} + \delta_{k,j} \tag{4.3}$$

and $m_{k+1,0} = m_{k,j}$.

The size of an event is given by the number of boxes N_f that participate in the event. All results presented here are taken after the system becomes statistically stationary. The statistical behavior of the system does not depend on the initial state except for a few special cases. Frequency–size statistics for $\alpha = 1$ and square arrays ($m = n$) of varying size ($n = 20$, 30, 40, 50) are given in Fig. 17. For smaller events ($1 < N_f < 10$) we have a power-law (fractal) dependence of $\log(N/N_0)$ on N_f, where N is the number of events with N_f blocks participating and N_0 is the total number of events studied. In out case $N_0 = 10{,}000$. In this range we find $N \sim N_f^{-1.57}$; the corresponding dashed line is given in Fig. 17. There are relatively fewer large events ($N_f > 10$). We see that the probability of an event of a given size does not appear to depend on the size of the array if the array is sufficiently large.

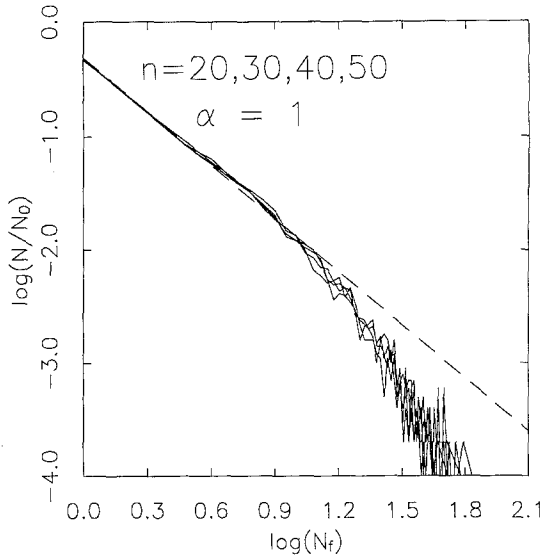

Fig. 17. Dependence of the fraction of events N/N_0 on size N_f for $\alpha = 1$ and several values of n. The dashed line is $N \sim N_f^{-1.57}$.

Frequency–size results for $\alpha = 5$ are given in Fig. 18. Again we have a power-law dependence for smaller events ($1 < N_f < 20$), with relatively fewer large events. The smaller events correlate with the relation $N \sim N_f^{-1.21}$. Frequency–size results for $\alpha = 50$ are given in Fig. 19. In this case the system is considerably stiffer and the relative number of large events is higher. We note an anomalously large number of catastrophic events in which all elements fail. The spike at $N_f = 400$ ($\log N_f = 2.60$) corresponds to catastrophic events with $n = 20$ and the spike at $N_f = 900$ ($\log N_f = 2.95$) corresponds to catastrophic events with $n = 30$. There are relatively few catastrophic events with $n = 40$ and 50. Except for the catastrophic events, the correlation with the power-law relation $N \sim N_f^{-1.26}$ is excellent.

We will now find the Lyapunov exponent using (2.30). Let $e_i^{0,0}$ be the initial forces and $e_i^{0,0'} = e_i^{0,0} + \Delta_i$ a random variation of the initial value, so we have two trajectories in the force phase space; $\Delta = (\Delta_1, \Delta_2, ..., \Delta_N)$ is a vector-column of the initial difference between two trajectories and its length $|\Delta|$ is the initial distance between two trajectories. Denote by

$$P_k = \mathrm{Jac}(L_{m_k, s_k})$$

the matrix of partial derivatives of the loading map introduced in (2.23), where s_k is the number of slips inside event k, and by

$$Q_{k,j} = \mathrm{Jac}(S_{m_k, j})$$

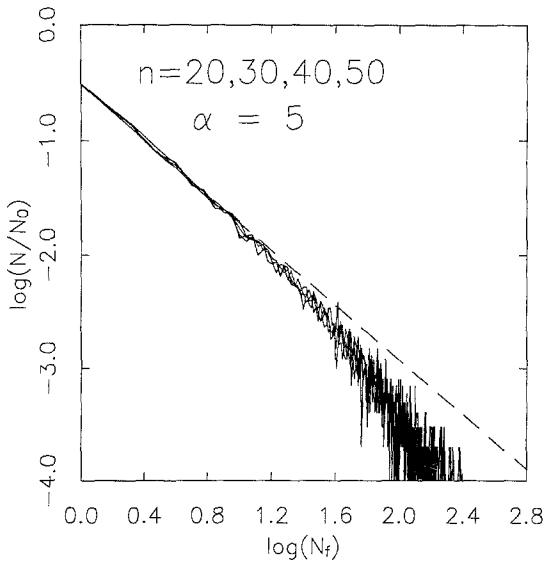

Fig. 18. Dependence of the fraction of events N/N_0 on size N_f for $\alpha = 5$ and several values of n. The dashed line is $N \sim N_f^{-1.21}$.

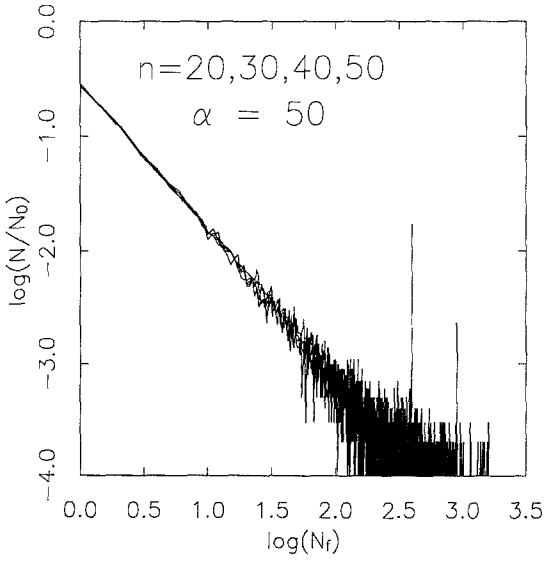

Fig. 19. Dependence of the fraction of events N/N_0 on size N_f for $\alpha = 50$ and several values of n. The spikes at $\log N_f = 2.60$ and 2.95 correspond to catastrophic events in which all blocks participate for $n = 20$ and $n = 30$, respectively.

the matrix of partial derivatives of the slip map introduced in (2.22). After the strain accumulation we have, using (2.28), the following distance between our two trajectories:

$$|\mathbf{e}^{1,0'} - \mathbf{e}^{1,0}| = |\Delta^{1,0}| = |P_0 \Delta| \tag{4.4}$$

so the distance between the trajectories increases in $\Lambda(0) = |P_0\Delta|/|\Delta|$ times. After the first slip in the first event we have, using (2.28) and (2.27),

$$|\mathbf{e}^{1,1'} - \mathbf{e}^{1,1}| = |\Delta^{1,1}| = |Q_{1,1}\Delta^{1,0}| = |Q_{1,1}P_0\Delta| \tag{4.5}$$

so the distance between the trajectories increases in $|Q_{1,1}P_0\Delta|/|\Delta|$ times. After the first event

$$|\mathbf{e}^{1,s_1'} - \mathbf{e}^{1,s_1}| = |\Delta^{1,s_1}| = |Q_{1,s_1} \cdots Q_{1,1}P_0\Delta| \tag{4.6}$$

Before the second event the distance between trajectories increases in

$$\Lambda(1) = |\mathbf{e}^{2,0'} - \mathbf{e}^{2,0}|/|\Delta| = P_1 Q_{1,s_1} \cdots Q_{1,1}P_0\Delta|/|\Delta| \tag{4.7}$$

times and so on. Before event $k+1$ the distance between trajectories becomes in $\Lambda(k)$ times more than the initial distance, where

$$\begin{aligned}\Lambda(k) &= |\mathbf{e}^{k+1,0'} - \mathbf{e}^{k+1,0}|/|\Delta| \\ &= |P_k Q_{k,s_k} \cdots Q_{k,1}P_k Q_{k-1,s_{k-1}} \cdots Q_{1,s_1} \cdots Q_{1,1}P_0\Delta|/|\Delta|\end{aligned} \tag{4.8}$$

To find the Lyapunov exponent, we should find the maximum possible value of $\Lambda(k)$ over all $\Delta \in \mathbf{R}^N$ [see (2.29) and (2.30)]; it gives us the maximum possible value of the ratio of the distance between two close trajectories before event $k+1$ and the initial distance over all possible pairs of close trajectories. We do not obtain the maximum for different Δ, as it is extremely difficult for large arrays (the dimension of the phase space is too large), but take arbitrary Δ. Then $\Lambda(k)$ gives us the increase of the distance between two arbitrary trajectories, which is less than the maximum possible value. We define $y \log \lambda_k = (1/k) \log \Lambda(k)$. The limit of λ_k as $k \to \infty$ gives us a lower bound for the Lyapunov exponent.

The dependence of λ_k on k for periodic boundary conditions, $\alpha = 1.4$ and $n = 10$, is given in Fig. 20. It is similar to Fig. 17. With periodic boundary conditions there is a region in phase space where we have periodic solutions. The periodic trajectory consists of single-slip events and all blocks slide consecutively in some order as in the symmetric case $\beta = 1$ for the two-block model. There is no such solution for free boundary conditions. The size of the periodic evolution region decreases with increasing α. Just as in the case of the two-block model with $\beta = 1$ the

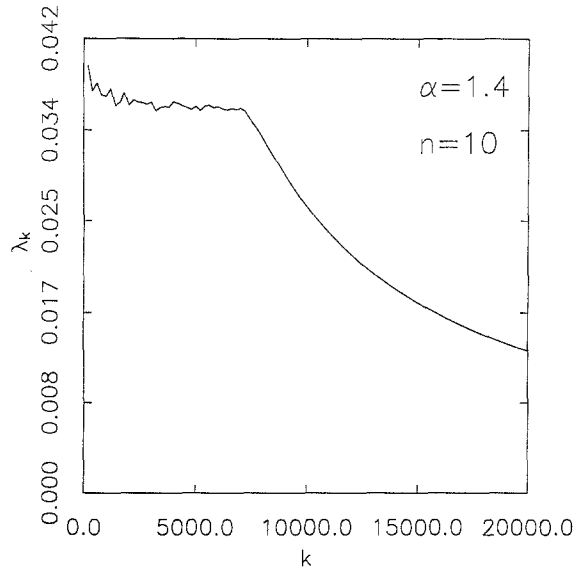

Fig. 20. Dependence of λ_k on k for periodic boundary conditions, $\alpha = 1.4$, and $n = 10$.

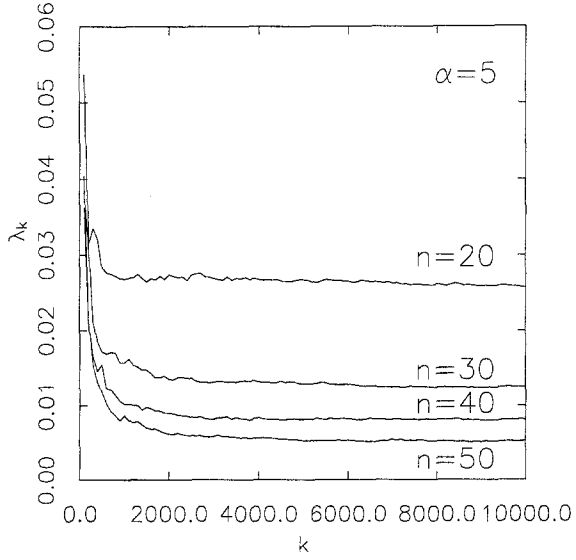

Fig. 21. Dependence of λ_k on k for free boundary conditions, $\alpha = 5$, and various values of n.

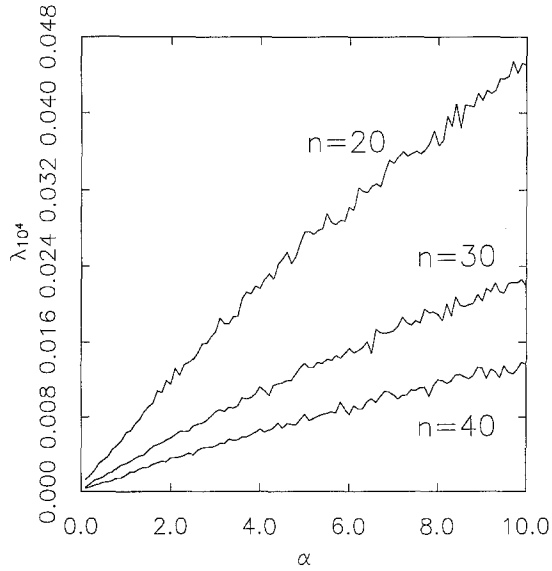

Fig. 22. Dependence of λ_{10^4} on α for several values of n.

evolution is chaotic until the trajectory intersects the periodic region. Intervals of chaotic behavior can be quite large for large numbers of blocks and large values of α; it can be more than 100,000 steps (see Fig. 20). In this case λ_k approaches 0 as $k \to \infty$ and the Lyapunov exponent is equal to 0.

The dependence of λ_k on k for free boundary conditions, $\alpha = 5$, and different sizes of the lattice ($n = 20$, 30, 40, 50) is given in Fig. 21. We see that we have positive Lyapunov exponents and they decrease with increasing lattice size.

The dependence of $\lambda_{10,000}$ on α different lattice sizes is given in Fig. 22. We can see that the Lyapunov exponent linearly increases with α, and so with increasing stiffness of our system it becomes more chaotic.

It is of interest to compare our results in which only one block is allowed to slide at one time with previous results in which large numbers of blocks are allowed to slide simultaneously.[5] The statistical behavior seems to be quite similar as well as the transition to the behavior with the slip of all blocks when the system becomes stiff.

5. DISCUSSIONS AND CONCLUSIONS

In this paper we have considered a slider-block model that strongly resembles a cellular automaton. We only allow one block to slip at a time

and consider only nearest neighbor interactions. Both low-order and high-order versions give interesting dynamical systems behavior.

In order to examine the low-order behavior of the system, we consider a pair of slider blocks connected to each other and to a constant-velocity driver with springs. The system is fully deterministic and an analytic expression can be written for the motion of each slider block. The termination of each slip is also deterministic since it occurs when the velocity of the block is zero. Each slip has a "memory" of its initial conditions; this is a necessary condition for chaotic behavior. Once the system has been set in motion no stochastic or noise components are introduced.

For a symmetric pair of slider blocks we always have periodic behavior, but the trajectory depends upon the initial conditions. If the system is asymmetric, a greater variety of behavior is found. For some parameter values the system behaves chaotically for all initial conditions. For other parameter values the behavior is chaotic for some initial conditions and evolves into periodic behavior for other initial conditions. For some parameter values the system evolves into a limit-cycle behavior that is independent of initial conditions. We have shown that the Lyapunov exponent is positive for the regime of chaotic behavior. The behavior is essentially similar to that obtained when both blocks are allowed to slide at once.[4]

In order to examine the behavior of high-order systems, we consider a square array composed of $N = n^2$ blocks. We assume complete symmetry so that the only parameters are the ratio of connecter spring constant to driver spring constant α and the array size n. This model is essentially a cellular automaton. The driver is allowed to move until the stability criterion on a single block is violated. This block undergoes simple harmonic motion and sticks when its velocity is first zero. The stored elastic energy in the driver spring is partially transferred to the adjacent blocks. If this transfer induces failures in one or more of the adjacent blocks, these are allowed to slip one at a time. Additional slips are allowed to occur until all blocks are stable.

The size of the slip event is specified by the number of boxes N_f that slip. Frequency–size statistics are obtained for a number of parameter values. In all cases we observe a power-law (fractal) dependence of number on size for the smaller events. If α is smaller than n, we find relatively few large events; the number of large events falls below the power-law correlation for small events. If α is larger than n, the system is relatively stiff and we find a relatively large number of catastrophic events that include all blocks. In all examples studied we have found positive Lyapunov exponents. We find that the exponent decreases toward zero for increasing size of the array n and increases for increasing stiffness (large α).

Applications of low-order systems that exhibit deterministic chaos have been limited. However, a variety of problems are directly applicable to higher-order systems. One of these is distributed seismicity. The original studies of slider-block systems[3] were motivated by the desire to understand earthquakes. Probably the most universal feature of earthquakes is that they satisfy Gutenberg–Richter frequency–magnitude statistics. Aki[9] has shown that the number of earthquakes with a rupture area greater than a specified value has a power-law dependence on the area. Within observational errors the fractal dimension is nearly always in the range $1.6 < D < 2$.

Because of this dependence a number of authors[6,10,11] have suggested that distributed seismicity is an example of self-organized criticality. There is a reasonable analog between the slip events in our model and earthquakes. The slip of the block over the surface is analogous to the displacements on a fault during an earthquake. The energy stored in the driver springs is analogous to the elastic energy stored in the rocks adjacent to a fault. This energy fluctuates as slip events (earthquakes) occur.

Keilis-Borok[12] has utilized pattern-recognition algorithms in successfully predicting earthquakes, including the 1988 Armenian and 1989 Loma Prieta earthquakes. The pattern recognition included seismic quiescence, increases in the clustering of earthquakes, and changes in aftershock statistics. Apparently there are systematic changes in the statistics of the smaller earthquakes prior to the occurrence of a large earthquake. These changes appear to occur over distances that are relatively large compared with the rupture area of the large earthquake. One objective of our studies of analog systems such as that given in this paper is to search for precursory statistical phenomena.

ACKNOWLEDGMENTS

We acknowledge stimulating discussions with Per Bak, John Rundle, and William Newman. This research was supported by the National Aeronautics and Space Administration under grant NAG 5-319. This is contribution #859 of the Department of Geological Sciences, Cornell University.

REFERENCES

1. E. N. Lorentz, *J. Atmos. Sci.* **20**:130 (1963).
2. P. Bak, C. Tang, and K. Wiesenfeld, *Phys. Rev.* **38A**:364 (1988).
3. R. Burridge and L. Knopoff, *Seis. Soc. Am. Bull.* **57**:341 (1967).
4. J. Huang and D. L. Turcotte, *Geophys. Res. Lett.* **17**:223 (1990).

5. J. M. Carlson and J. S. Langer, *Phys. Rev.* **40A**:6470 (1989).
6. K. Ito and M. Matsuzaki, *J. Geophys. Res.* **95**:6853 (1990).
7. H. Nakanishi, *Phys. Rev.* **41A**:7086 (1990).
8. S. R. Brown, C. H. Scholz, and J. B. Rundle, *Geophys. Res. Lett.* **18**:215 (1991).
9. K. Aki, in *Earthquake Prediction*, D. W. Simpson and P. G. Richards, eds. (American Geophysical Union, Washington, D.C., 1981).
10. P. Bak and C. Tang, *J. Geophys. Res.* **94**:15635 (1989).
11. A. Sornette and D. Sornette, *J. Europhys. Lett.* **9**:197 (1989).
12. V. I. Keilis-Borok, *Rev. Geophys.* **28**:19 (1990).